Excellent p-n control in a high temperature thermoelectric boride

Satofumi Maruyama, Yuzuru Miyazaki, Kei Hayashi, Tsuyoshi Kajitani, and Takao Mori

Articles you may be interested in

Magnetic and magnetocaloric properties of the new rare-earth–transition-metal intermetallic compound Gd3Co29Ge4B10
J. Appl. Phys. **111**, 07E333 (2012); 10.1063/1.3677658

Enhancement of thermoelectric efficiency in type-VIII clathrate Ba 8 Ga 16 Sn 30 by Al substitution for Ga
J. Appl. Phys. **108**, 073705 (2010); 10.1063/1.3490776

High temperature thermoelectric transport properties of p -type Ba 8 Ga 16 Al x Ge 30 − x type-I clathrates with high performance
J. Appl. Phys. **103**, 073503 (2008); 10.1063/1.2902504

Electrical transport and thermoelectric properties of Y 1 − x Ca x Co O 3 (0 x 0.1) at high temperatures
J. Appl. Phys. **101**, 083709 (2007); 10.1063/1.2721381

High temperature thermoelectric properties of B 12 icosahedral cluster-containing rare earth boride crystals
J. Appl. Phys. **97**, 093703 (2005); 10.1063/1.1883726

Excellent p-n control in a high temperature thermoelectric boride

Satofumi Maruyama,[1,2] Yuzuru Miyazaki,[2] Kei Hayashi,[2] Tsuyoshi Kajitani,[2] and Takao Mori[1,3,a]

[1]National Institute for Materials Science (NIMS), 1-1 Namiki, Tsukuba 305-0044, Japan
[2]Department of Applied Physics, Graduate School of Engineering, Tohoku University, 6-6-05 Aoba, Aramaki, Aoba-ku, Sendai 980-8579, Japan
[3]University of Tsukuba, 1-1-1 Tennodai, Tsukuba, Ibaraki 305-8577, Japan

Polycrystalline samples of $Y_xAl_yB_{14}$ ($x \sim 0.57$) with different fractional occupancies y ($0.41 \leq y \leq 0.63$) were synthesized and their thermoelectric properties investigated. Electrical conductivities generally followed three-dimensional variable range hopping with a rapid delocalization indicated as electrons were increased. Positive Seebeck coefficients were obtained for the Al-poor sample, $y = 0.41$, which was shifted in the negative direction with increase of y. Maximum Seebeck coefficient values were approximately $400 \, \mu V \, K^{-1}$ at 850 K and $-200 \, \mu V \, K^{-1}$ at 1000 K, for p-type and n-type, respectively. Excellent control of p-n characteristics was achieved in a system with the same crystal structure and consisting of the same elements. © 2012 American Institute of Physics. [http://dx.doi.org/10.1063/1.4758297]

There has been great interest in research of thermoelectric materials, for the urgent green energy harvesting[1,2] from factory and incinerator waste heat, and focused solar power, for example.

Boron-rich cluster compounds possess covalently bonded boron networks. Through incorporation of rare earth or other metal atoms and third elements like C, N, and Si in the framework, chemical and physical properties can be controlled.[3] In addition to this, they generally have attractive thermal and chemical stabilities. Furthermore, as an important aspect for thermoelectrics, the boron icosahedral cluster compounds are known to generally exhibit intrinsic low thermal conductivity.[4–7]

For example, boron carbide is a good p-type high temperature thermoelectric compound[8,9] and is one of the few commercialized thermoelectric materials. However, due to the need for well matching p- and n-type legs, one long standing problem for boron carbide was the lack of a good n-type counterpart since boron icosahedral compounds have been found to be predominantly p-type. Therefore, various rigorous attempts have been made over the years to obtain n-type boron cluster compounds.[10–12] Recently, a potential n-type counterpart to boron carbide was discovered in the homologous borocarbonitride series of $RB_{17}CN$ and $RB_{22}C_2N$.[13,14] However, the processing of these compounds is difficult, and the thermoelectric properties still need to be improved.

In this work, we have focused on a different boron cluster system and, through synthesis techniques, have been able to achieve excellent p-n control with large absolute values of the Seebeck coefficient, by using the same constituent elements. We started from $YAlB_{14}$ (Refs. 15 and 16) and YB_{25} (Ref. 17), which have boron icosahedra clusters forming similar network structures. Korsukova reported a crystal structure model based on the single crystal x-ray diffraction (XRD) measurement for $YAlB_{14}$, which was prepared using high temperature molten Al flux method, with a refined composition of $Y_{0.62}Al_{0.71}B_{14}$. Y and Al atoms occupy the interstitial position partially in B network containing B_{12} icosahedra as shown in Fig. 1. However, details on the thermoelectric properties have not been fully investigated, and only a narrow composition range has been elucidated.[15,16] We were able to synthesize $YAlB_{14}$ with different Al occupancies and found striking thermoelectric properties.

Polycrystalline samples of $Y_xAl_yB_{14}$ ($x \sim 0.57$) were obtained in Al flux. Starting materials of YB_4 (99.9%, Japan New Metals Co., Ltd.), B (99%, New metals and chemicals, Ltd.), and excess Al, serving as flux (99%, Wako Pure Chemical Industries, Ltd.) were mixed with nominal composition of $Y_{0.56}Al_yB_{14}$ ($y = 2.8$–5.6).

These mixtures were pressed using cold isostatic press (CIP) and sintered in Ar atmosphere or vacuum. Samples sintered in Ar gas were heated at 1400 °C for 12 h in an electrical furnace. Samples sintered in vacuum were wrapped in Ta tubes and heated in a range of 1400 °C–1500 °C to investigate control of Al occupancy through evaporation. All samples were heated for 8 h using an induction furnace. After sintering, these samples were crushed and washed in NaOH to dissolve the excess Al.
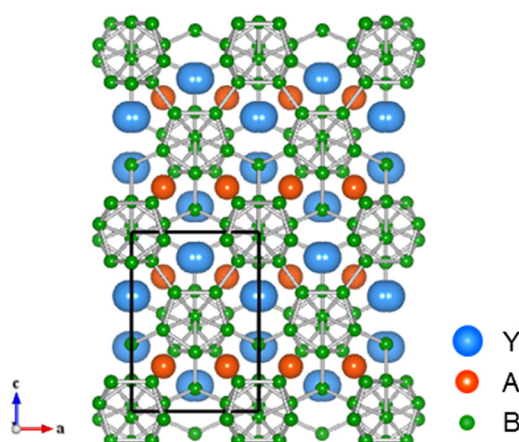

FIG. 1. Crystal structure of $Y_xAl_yB_{14}$.

a)Author to whom correspondence should be addressed. Electronic mail: MORI.Takao@nims.go.jp. Tel.: +81-29-860-4323. Fax: +81-29-851-6280.

TABLE I. Details of synthesis of the $Y_xAl_yB_{14}$ sample fabricated through SPS treatment.

Molar ratio of starting material (Y:Al:B)	Sintering in furnace			SPS		Relative density (%)	y in $Y_xAl_yB_{14}$
	Atmosphere	Temperature (°C)	Hold time (h)	Temperature (°C)	Hold time (min)		
0.56:5.6:14	Argon	1400	12	1500	5	71.1	0.62
0.56:5.6:14	Argon	1400	12	1550	5	77.4	0.63
0.56:2.8:14	Argon	1400	12	1600	…	99.7	0.53
0.56:2.8:14	Vacuum	1500	8	1550	5	93.3	0.41
0.56:2.8:14	Vacuum	1400	8	1550	5	89.4	0.60

After these processes, samples were pressed at 80 MPa by using spark plasma sintering (SPS) for thermoelectric measurements. Samples sintered in Ar gas were pressed at different temperatures with a general holding time of 5 min. At 1600 °C, metallic droplets were observed, so the SPS process was stopped immediately. Synthesis conditions are summarized in Table I. XRD measurements using Rigaku Ultima-3 with Cu Kα radiation were performed to characterize the samples and to determine the detailed crystal structure by means of Rietveld refinement method using Rietan-FP software.[18] Electrical resistivity and Seebeck coefficient were measured with ULVAC ZEM-2 by using the four-probe method and differential method, respectively. To determine thermal conductivity, the thermal diffusivity coefficients were measured by the laser flash method, and the specific heat was measured by a Quantum Design PPMS.

XRD patterns of $Y_xAl_yB_{14}$ after the SPS process are shown in Fig. 1. Although small amounts of Al_2O_3 or YB_6 were detected, we obtained polycrystalline $Y_xAl_yB_{14}$ samples. The fractional occupancy y in $Y_xAl_yB_{14}$ was estimated and shown in Figs. 2(b) and 2(c). By sintering in vacuum, samples with different Al occupancies were synthesized as shown in Fig. 2(c), while little difference was observed when sintering in Ar gas (Fig. 2(b)). By sintering in vacuum, evaporation of Al enabled Al desorption. With increase of sintering temperature, desorption of Al in $YAlB_{14}$ was promoted because saturated vapor pressure of Al is 10 Pa (vacuum of

our chamber during this synthesis) at about 1360 °C. Now we consider the effect of the SPS treatment. For the sintering done in vacuum, the y values were almost the same before and after SPS (Fig. 2(c)), while y for the samples sintered in Ar gas generally shows a slight decrease, with a large drop for the sample with SPS done at 1600 °C in which droplets were observed to come out (Fig. 2(b)).

We list the number of valence electrons contributed from Y^{3+} and Al^{3+} in Table II. The occupation numbers of Y^{3+} and Al^{3+} were determined from Rietveld refinement calculation. A typical composition reported for the previous single crystal samples, $Y_{0.62}Al_{0.71}B_{14}$, is equivalent to 3.99 electrons from Y^{3+} and Al^{3+}. With our synthesis, we were able to largely modify the Al occupancies and thereby modify the number of valence electrons in these compounds.

Figure 3 shows the temperature dependence of the electrical resistivity. For Al-poor samples, large decreases of the resistivity were observed with increase of the temperature. Al-rich samples exhibited lower electrical resistivity relative to the Al-poor samples because of apparent delocalization of the carriers which will be described next.

For approximately the same Al occupancy, the denser sample exhibited lower electrical resistivity ($y = 0.60$, $y = 0.62$ versus $y = 0.63$), as was expected.

Most of the borides consisting of B_{12} icosahedra clusters have been found to follow Mott's variable range hopping mechanism for three dimensional systems[19,20]
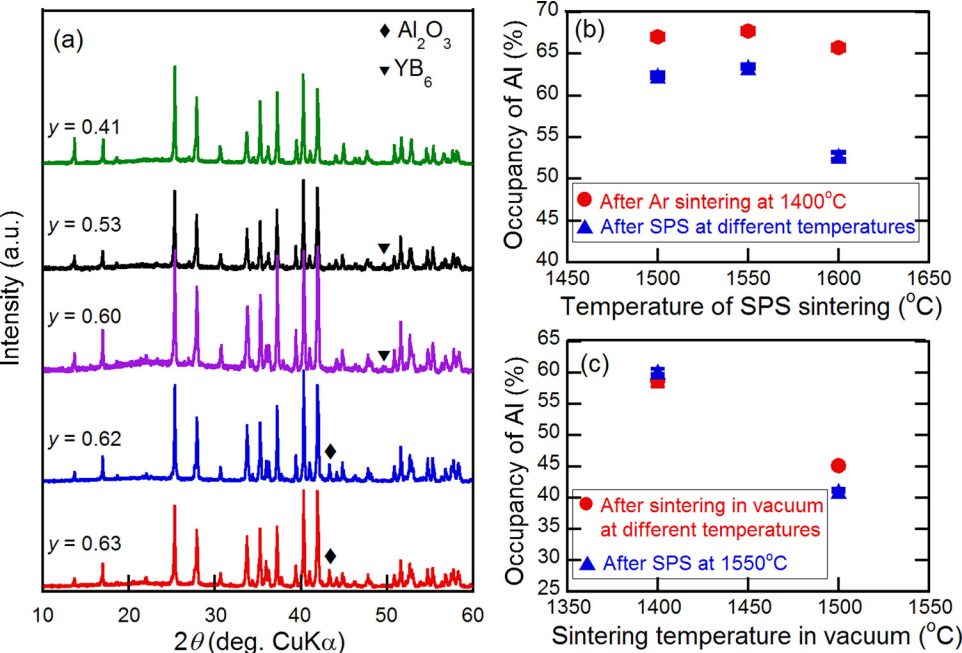

FIG. 2. (a) Powder XRD pattern of $Y_xAl_yB_{14}$ ($x \sim 0.57$) after SPS treatment, and Al occupancy dependence on the (b) SPS sintering temperature (for the samples originally sintered in Ar at 1400 °C) and (c) sintering temperature (for the samples originally sintered in vacuum).

TABLE II. The number of valence electrons from Y and Al atoms.

Sample	Composition	Number of electrons
$y = 0.41$	$Y0.57Al0.41B14$	2.96
$y = 0.53$	$Y0.54Al0.53B14$	3.23
$y = 0.60$	$Y0.55Al0.60B14$	3.47
$y = 0.62$	$Y0.51Al0.62B14$	3.40
$y = 0.63$	$Y0.52Al0.63B14$	3.47

TABLE III. Characteristic temperature and γ coefficient of specific heat in $Y_xAl_yB_{14}$.

Sample	T_0 (K)	γ (mJ/mol K^2)
$y = 0.41$	1.6×10^8	0.46
$y = 0.60$	2.5×10^3	0.61

$$\rho = \rho_0 \exp[(T_0/T)^{0.25}]. \tag{1}$$

T_0 is the so-called characteristic temperature and follows the relationship

$$k_B T_0 = 1.5/[D(E_F)\xi^3], \tag{2}$$

where $D(E_F)$ is the density of states at the Fermi level and ξ is the localization length.[20]

From a fit of our data to Eq. (1), we determined a T_0 value of 1.6×10^8 K for $y = 0.41$ and 2.5×10^3 K for $y = 0.60$. Considering Korsukova's report that T_0 of $Er_{0.62}Al_{0.73}B_{14}$ was 670 K below room temperature, the increase of Al occupancy seems to lead to rapid decrease of the T_0 value (Table III). To evaluate the localization length, we carried out low temperature specific heat measurement to estimate $D(E_F)$ from the γ coefficients, which are given in Table III. Localization lengths ξ are determined from Eq. (2) to be 0.94 Å for $y = 0.41$, and 34.1 Å for $y = 0.60$. Although there can be some effects from differences in density, from the large differences obtained for ξ, it can be inferred that there is a rapid delocalization as Al is increased, i.e., the number of valence electrons is increased.

Figure 4(a) shows the temperature dependence of the Seebeck coefficient. The Al-poor sample, $y = 0.41$, exhibited positive values with a maximum value of around 400 $\mu V/K$ at 850 K. However, the Seebeck coefficient showed a large negative shift with increase of the Al occupancy, and the Al-rich samples ($y = 0.60, 0.62$, and 0.63) exhibited negative values of approximately $-200 \mu V/K$ at 1000 K. The Seebeck coefficient in variable-range hopping has been investigated, for example, by Zvyagin.[21] Assuming a linear density of state, the Seebeck coefficient has the following dependency:
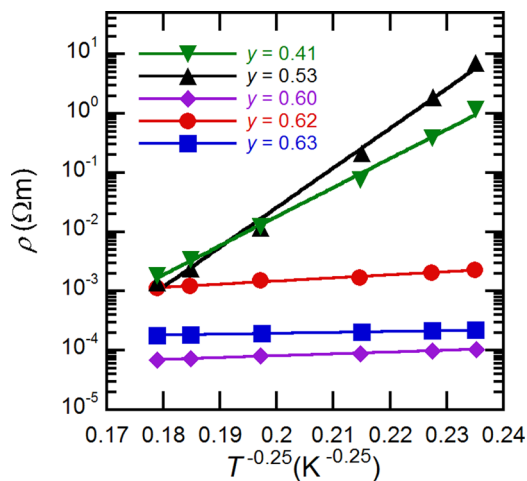
$$S \propto T^{1/2}. \tag{3}$$

Although there is a minor deviation as the Seebeck coefficient of the Al-poor sample appears to saturate at a broad maximum around 850 K, the absolute values of S in the Al-rich samples continue to increase with increasing temperature and the curves are approximately proportional to $T^{1/2}$, indicating that these systems are following the hopping transport.

Figure 4(b) shows the Al occupancy y dependence of the Seebeck coefficient at 1000 K. Increase of the Al occupancy y is equivalent to a greater number of electrons being doped into the structure (Table II), and the Seebeck coefficient shifts from positive value to negative. It can be seen that the crossover from p- to n-type occurs around $y = 0.53$, i.e., 3.2 electrons doped. The bonding in compounds such as Mg_2B_{14} has been discussed previously,[22] and since the boron icosahedra is "2 electron deficient," the "B_{14}" in YAl_xB_{14}, i.e., $B \cdot B_{12} \cdot B$, can be considered to be 4 electron deficient. In this simple bonding picture, when more than 4 electrons are supplied, there is an excess of electrons. However, in $Y_xAl_yB_{14}$, we observe a crossover to n-type at 3.2 electrons ($y = 0.53$), which indicates that the bonding in this compound is different than expected from the simple picture.

FIG. 3. Temperature dependence of electrical resistivity of $Y_xAl_yB_{14}$ ($x \sim 0.57$). The logarithmic ρ is plotted versus $T^{-0.25}$.
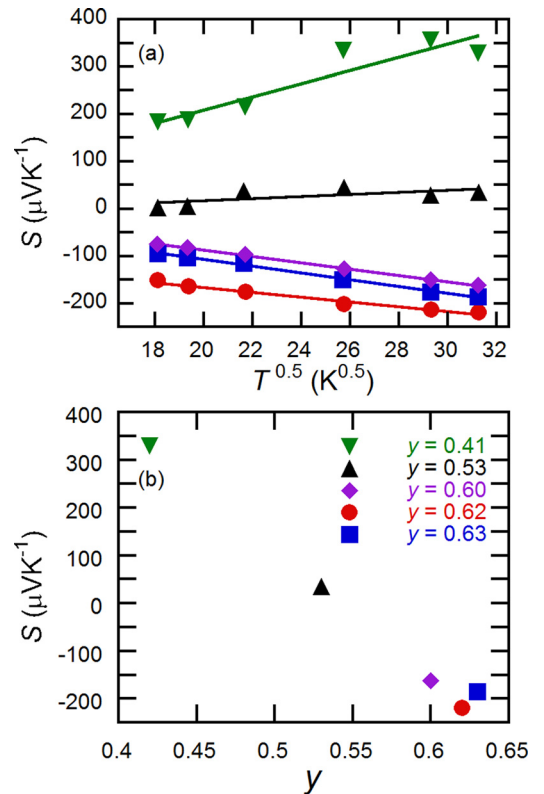

FIG. 4. Temperature dependence of the Seebeck coefficient (a) plotted versus $T^{0.5}$ and effect of Al occupancy y on the Seebeck coefficient measured at 1000 K.
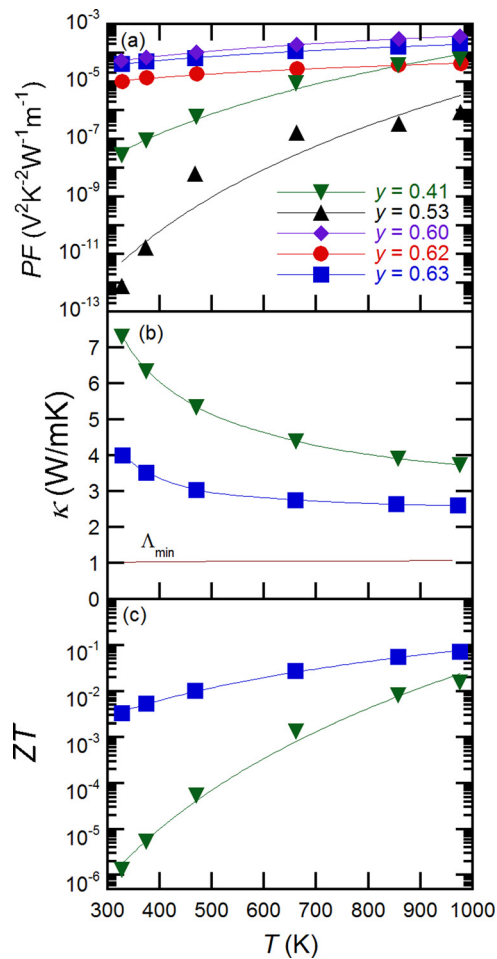
FIG. 5. Temperature dependence of the (a) power factor, *PF*; (b) thermal conductivity, κ; and (c) *ZT*. The estimated minimum thermal conductivity Λ_{min} (Ref. 23) is also plotted.

The non-icosahedral B sites should most likely be considered more carefully, and this will be further investigated in the near future with theoretical methods. To summarize, we have been able to make $Y_xAl_yB_{14}$ alloys that have either strong p- or n-type thermoelectric properties by controlling the occupancy of Al.

Figure 5(a) shows the temperature dependence of the power factor. The power factors increase with increase of the temperature. Maximum values of p type and n type materials are 5.9×10^{-5} V^{-2} K^{-2} Ω^{-1} m^{-1} and 3.8×10^{-4} V^{-2} K^{-2} Ω^{-1} m^{-1}, respectively.

The temperature dependence of the thermal conductivities of the $y = 0.41$ and 0.63 samples is shown in Fig. 5(b). The thermal conductivities decrease with increase of temperature and take values around 3 to 4 W/mK at 1000 K. Cahill *et al*. have previously made a treatment of disordered solids and demonstrated a lower limit to the thermal conductivity, Λ_{min}, which is approached in highly disordered cases.[23] We follow their method and for reference, plot Λ_{min} which we have calculated using estimated parameters of the x = 0.63 sample (number density of atoms was $n = 1.2 \times 10^{23}$ cm^{-3}, while we estimate the speed of sound from specific heat data as 2.1 km/s and 3.6 km/s for transverse and longitudinal speeds, respectively, assuming a relationship as given previ-

ously[24]). Λ_{min} is substantially smaller than the measured values, which agrees with the indicated crystalline temperature dependence, which points to disorder not being so largely dominant in this system. We used the thermal conductivity values to estimate the figure of merit *ZT* and plotted this in Fig. 5(c). Maximum values of p type and n type materials are 0.015 and 0.072, respectively. The *ZT* values are still low due to the poor electrical resistivity, which can be partly attributed to non-optimal densities of the samples. With further optimization of the SPS condition and also the Al occupancies, further improvements are expected.

In this study, polycrystalline samples of $Y_xAl_yB_{14}$ with different fractional occupancies *y* were synthesized by controlling synthesis conditions, and their thermoelectric properties were investigated. The Seebeck coefficients were shifted from positive values to negative values with the increase of the fractional occupancy *y* in $Y_xAl_yB_{14}$, with maximum values of approximately 400 μV K^{-1} at 850 K and -200 μV K^{-1} at 1000 K, for p- and n-type, respectively. This is quite striking since we have achieved good control over strong p- or n-type characteristics in a thermoelectric material with the same crystal structure and composed of the same, relatively abundant constituent elements.

[1]*Thermoelectrics: Basic Principles and New Materials Development*, edited by G. S. Nolas, J. Sharp, and H. J. Goldsmid (Springer, Berlin, 2001).

[2]*Chemistry, Physics and Materials Science of Thermoelectric Materials: Beyond Bismuth Telluride*, edited by M. G. Kanatzidis (Kluwer, 2003).

[3]T. Mori, in *Handbook on the Physics and Chemistry of Rare-Earths*, edited by K. A. Gschneidner, Jr., J.-C. Bunzli, and V. Pecharsky (North-Holland, Amsterdam, 2008), Vol. 38, p. 105.

[4]D. G. Cahill, H. E. Fischer, S. K. Watson, R. O. Pohl, and G. A. Slack, Phys. Rev. B **40**, 3254 (1989).

[5]T. Mori, Physica B **383**, 120 (2006).

[6]T. Mori, J. Martin, and G. Nolas, J. Appl. Phys. **102**, 073510 (2007).

[7]T. Mori, in *Modules, Systems, and Applications in Thermoelectrics*, edited by D. M. Rowe (CRC, London, 2012), p. 14.

[8]C. Wood and D. Emin, Phys. Rev. B **29**, 4582 (1984).

[9]T. L. Aselage, D. Emin, S. S. McCready, and R. V. Duncan, Phys. Rev. Lett. **81**, 2316 (1998).

[10]R. Schmechel and H. Werheit, J. Phys. Condens. Matter **8**, 7263 (1996).

[11]G. A. Slack, J. H. Rosolowski, C. Hejna, M. Garbauskas, and J. S. Kasper, in *Proceedings of the 9th International Symposium on Boron, Borides and Related Compounds, Duisberg, Germany* (Univ. Duisberg, 1987), p. 132.

[12]S. Balaz, D. I. Dimov, N. M. Boag, K. Nelson, B. Montag, J. I. Brand, and P. A. Dowben, Appl. Phys. A **84**, 149 (2006).

[13]T. Mori and T. Nishimura, J. Solid State Chem. **179**, 2908 (2006).

[14]T. Mori, T. Nishimura, K. Yamaura, and E. Takayama-Muromachi, J. Appl. Phys. **101**, 093714 (2007).

[15]M. M. Korsukova, V. N. Gurin, Yu. B. Kuzma, N. F. Chaban, S. I. Chykhrii, V. V. Moshchalkov, N. B. Brandt, A. A. Gippius, and K. K. Nyan, Phys. Status Solidi A **114**, 265 (1989).

[16]M. M. Korsukova, T. Lundstrom, L.-E. Tergenius, and V. N. Gurin, J. Alloys Compd. **187**, 39 (1992).

[17]T. Mori, F. X. Zhang, and T. Tanaka, J. Phys.: Condens. Matter **13**, L423 (2002).

[18]F. Izumi and K. Momma, Solid State Phenom. **130**, 15 (2007).

[19]A. L. Efros and M. Pollak, *Electron-Electron Interactions in Disordered Systems* (North-Holland, Amsterdam, 1985), p. 409.

[20]N. F. Mott, J. Non-Cryst. Solids **1**, 1 (1968).

[21]I. P. Zvyagin, Phys. Status Solidi B **58**, 443 (1973).

[22]D. W. Bullett, J. Phys. C **15**, 415 (1982).

[23]D. G. Cahill, S. K. Watson, and R. O. Pohl, Phys. Rev. B **46**, 6131 (1992).

[24]J. F. Berret and M. Meissner, Z. Phys. B: Condens. Matter **70**, 65 (1988).